TABLE 1

A. Sequence of Oligonucleotide Primers Used for Sequencing of *MURC* Exons

(Genomic DNA Sequence Source: NC_000009.11, GI:224589821)

Exon 1 (nucleotides 5- 586)

Forward: 5'CCTGTTGCCTGTTATCAAGCTGAC3'

Reverse: 5'GACACTGGAAACCTCTGATATGAC3'

Exon 2 - Fragment 1 (nucleotides 7637 - 8058)

Forward: 5'CATGGCCAGAAGGTAAAAGAGCTG3'

Reverse: 5'CCTGACTGTCTCAGCCTCTCTC3'

Exon 2 - Fragment 2 (nucleotides 7930 - 8475)

Forward: 5'GACACGGCAGAATCTTGACAAG3'

Reverse: 5'CATGGCACAGAAATGTAGACGAC3'

B. Sequence of Oligonucleotide Primers Used for Mutagenesis

p.N128K

Forward: 5'GTCAAGCAAGAGGAAATAATGAAGAAAAAGAAATTCCGCGTGG3'

Reverse: 5'-CCACGCGGAATTTCTTTTTCTTCATTATTTCCTCTTGCTTGAC3'

p.R140W

Forward: 5'-CAGGAGAAGTTTTGGTGTCCGACATCCCTGTCTG3'

Reverse: 5'-CAGACAGGGATGTCGGACACCAAAACTTCTCCTG3'

p.L153P

Forward: 5'-GTCTGTTGTTAAAGACAGAAACCCAACTGAGAACCAAGAAGAGG3'

Reverse: 5'-CCTCTTCTTGGTTCTCAGTTGGGTTTCTGTCTTTAACAACAGAC3'

p.S307T

Forward: 5'-GTCTCTGGGCCCCATCACTGAGCTCTACTCTG3'

Reverse: 5'-CAGAGTAGAGCTCAGTGATGGGGCCCAGAGAC3'

p.P324L

Forward: 5'-GAACACGAGGCAGCCAGGCTGGTGTATCCTCCCCATGAAG3'

Reverse: 5'-CTTCATGGGGAGGATACACCAGCCTGGCTGCCTCGTGTTC3'

p.S364L

Forward: 5'-GATTTAAAGCACTCATTGGACTACAAAGACGATGACGAC3'

Reverse: 5'-GTCGTCATCGTCTTTGTAGTCCAATGAGTGCTTTAAATC3'

C. Sequence of Oligonucleotide Primers Used in qPCR

Rat atrial natriuretic peptide (ANP or *Nppa*)

Forward: 5'-ATACAGTGCGGTGTCCAACA-3'

Reverse: 5'-CGAGAGCACCTCCATCTCTC-3'

Rat brain natriuretic peptide (BNP or *Nppb*)

Forward: 5'-GGAAATGGCTCAGAGACAGC-3'

Reverse: 5'-CGATCCGGTCTATCTTCTGC-3'

Rat skeletal α-actin (SkA or *Acta1*)

Forward: 5'-CACGGCATTATCACCAACTG-3'

Reverse: 5'-CCGGAGGCATAGAGAGACAG-3'

Rat glyceraldehyde-3-phosphate dehydrogenase (*Gapdh*)

Forward: 5'-ATGGGAAGCTGGTCATCAAC-3'

Reverse: 5'-GTGGTTCACACCCATCACAA-3'

Online Supplementary Material

TABLE 2

Non-Synonymous Variants Identified in the Probands and Controls

Variants		Controls		DCM		HCM	
		N=509		N=383		N=307	
		AA	C	AA	C	AA	C
		316	193	179	204	49	258
AA	Nucleotide						
p.S20T	g. 149G>C	2	0	1	0	0	0
p.S78L	g.323C>T	13	0	6	1	2	0
p.N81K	g.333T>G	1	0	1	0	1	0
p.R131H	g.482G>A	1	2	2	1	0	0
p.D163G	g.7791A>G	9	0	4	0	1	0
p.R231K	g.7795G>A	2	0	0	0	1	0
Total number of non-synonymous variants per group and ethnic background		28	2	14	2	5	0
Total number of non-synonymous variants per group		30 (5.9%)		16 (4.2%)		5 (1.6%)	

The prevalence of these non-synonymous variants was not significantly different between the DCM probands and controls. Likewise, the mean and median ages of individuals with these rare non-synonymous variants in the control and the DCM groups were similar (mean: 48.7 ± 8.6 vs. 47.9 ± 3.9, respectively, p=0.537; median: 45 vs. 49 years; range: 22 to 81 vs. 23 to 72 years).

Online Supplementary Material

Table 3

Synonymous, non-coding and deletion variants identified in the study population

Study Population		Total	Control		DCM		HCM	
			AA	C	AA	C	AA	C
		1,199	316	193	179	204	49	258
Nucleotide	Amino acid	Number of Individuals with DNA Sequence variants						
		1,183	264	233	178	211	47	250
g.34G>A	Non-coding	10	1	3	3	2	1	0
g.34G>R	Non-coding	6	1	0	0	5	0	0
g.79G>R	Non-coding	1	0	0	1	0	0	0
g.147G>R	p.S19S	5	2	0	2	0	1	0
g.267G>R	p.R59R	1	0	1	0	0	0	0
g.339G>K	p.G83G	1	0	0	0	1	0	0
g.504C>M	Non-coding	11	4	0	7	0	0	0
g.507G>R	Non-coding	2	0	0	1	0	1	0
g.526T>Y	Non-coding	3	1	0	2	0	0	0
g.540T>C	Non-coding	75	10	21	7	13	2	22
g.540T>Y	Non-coding	361	96	75	43	63	10	74
g.7729G>R	p.P142P	1	0	0	0	0	1	0
g.7822G>S	p.S173S	1	0	0	0	0	0	1
g.7873A>T	p.S190S	1	0	0	1	0	0	0
g.7873A>W	p.S190S	81	26	8	25	5	6	11
g.7918A>R	p.E205E	3	2	0	1	0	0	0
g.7981G>K	p.V226V	1	0	0	1	0	0	0
g.7987G>R	p.P228P	1	0	0	1	0	0	0
g. 8005A>R	p.L234L	5	0	1	0	1	0	3
g. 8008G>R	p.R235R	6	0	2	0	1	0	3
g.8017A>R	p.G238G	1	0	1	0	0	0	0
g.8203C>Y	p.S300S	1	1	0	0	0	0	0
g.8299G>A	p.R332R	150	17	33	15	29	6	50
g.8299G>R	p.R332R	434	94	87	60	89	18	86
g.8427A>R	Non-coding	3	0	1	0	2	0	0
g.8444T>Y	Non-coding	18	9	0	8	0	1	0

Online Figure 1

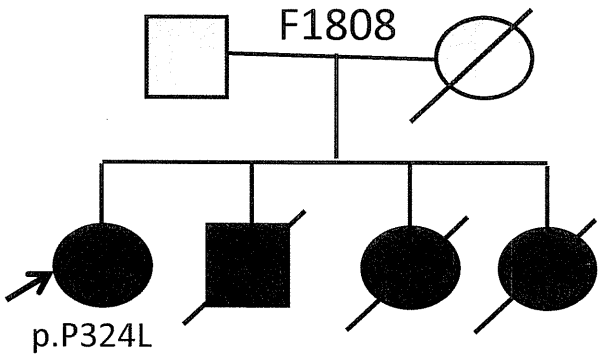

D9S180	231/233
D9S910	110/125
D9S176	151/153

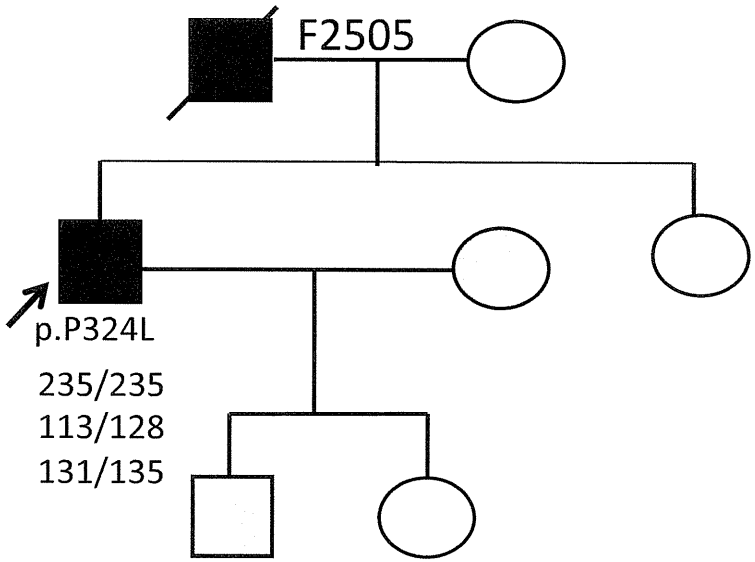

D9S180	235/235
D9S910	113/128
D9S176	131/135

D9S180	235/235
D9S910	110/113
D9S176	131/143

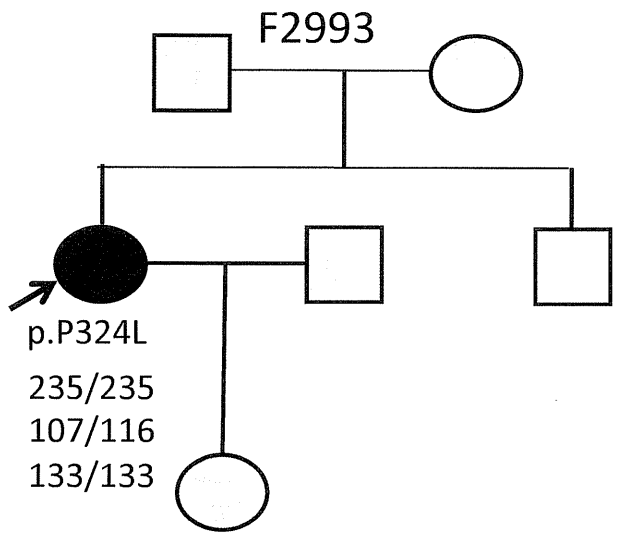

D9S180	235/235
D9S910	107/116
D9S176	133/133

Online Figure 2

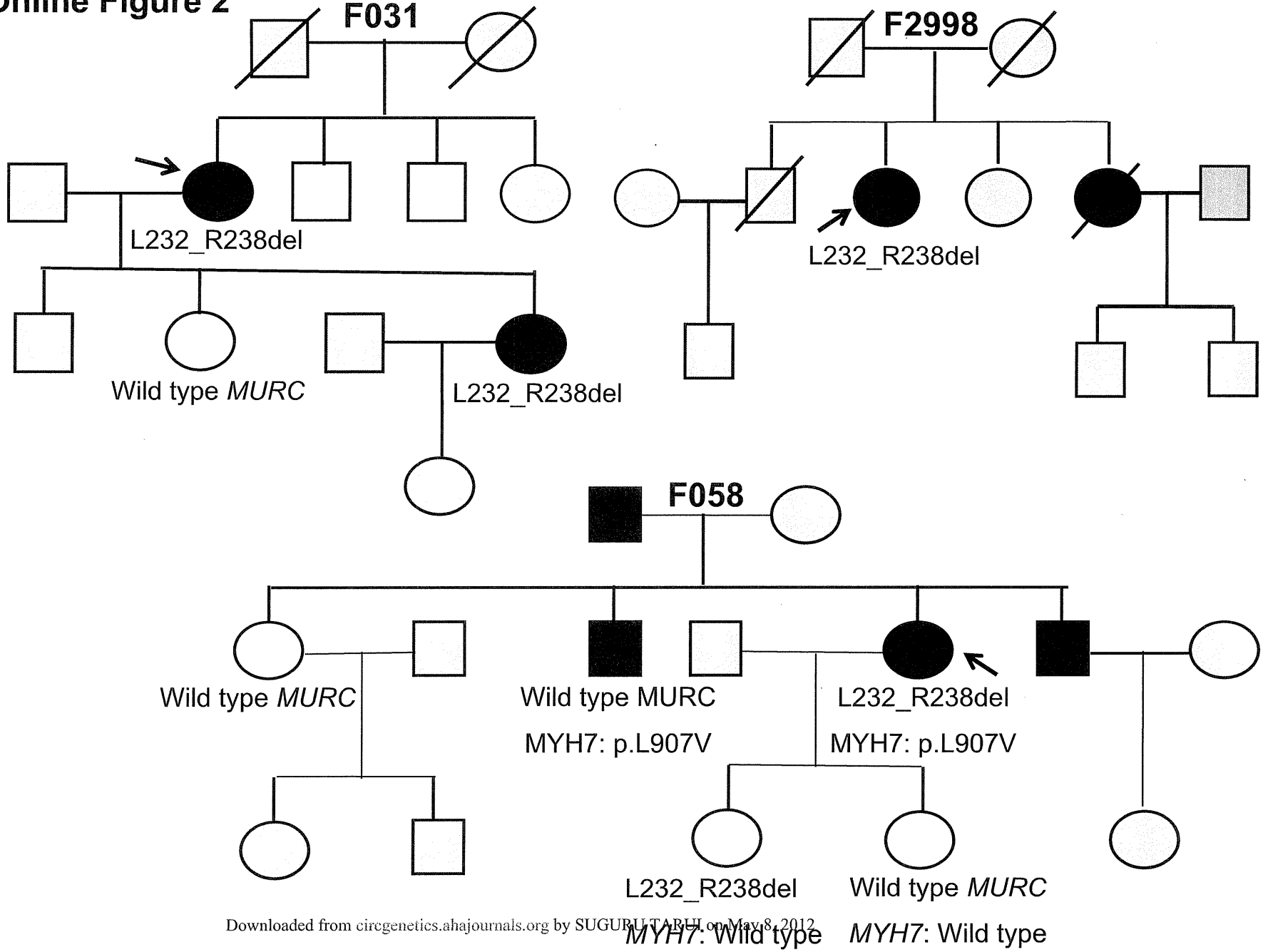

Supplemental figure legend

Supplemental Figure 1. Genotypes of three probands with familial dilated cardiomyopathy and the p.P324L variant in *MURC* gene, who were typed for three short tandem repeat markers at the *MURC* locus. As shown the probands do not share a common locus haplotypes, indicating an independent origin of the p.P324L variants in three probands. Pedigree symbols are per convention (full circles and squares indicate affected females and males respectively. Empty circles and squares indicate normal females and males respectively. Grey symbols indicate individuals that were not phenotyped.

Supplemental Figure 2. Detection of the deletion variant (L232-R238del) in three families with hypertrophic cardiomyopathy. The deletion variant did not co-segregate with the phenotype in Family F058 as one clinically affected family member did not have the deletion mutation. A second mutation p.L907V in MYH7 was detected in two affected members in this family. Symbols are as in Supplemental Figure 1.

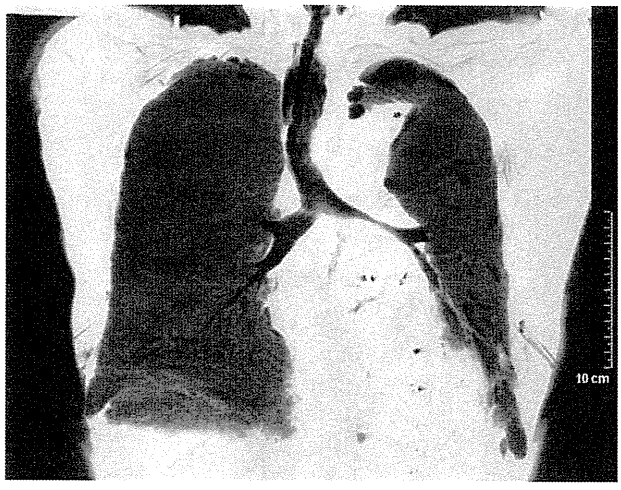

FIGURE 2. Minimum intensity projection showing compression of the left main bronchus. Minimum intensity projection demonstrates areas of lowest density, being equivalent to air. Other structures appear gray or black because of their density.

been described yet. Options could be open repair or dilatation with or without endobronchial stenting.

Madden, Loke, and Sheth[5] reported a series of 31 patients undergoing bronchial stenting for airway compression. Clinical outcome was poor owing to obstructing granulation, mucus plugging, recurrent respiratory infections, and stent migration/fracture. Thus the value of stenting in airway compression is questionable and at best represents a palliative treatment. Another conceivable option for such patients is surgery. However, nothing has been reported so far, but a higher surgical risk can be anticipated owing to the potential for severe bleeding. In this case, to our understanding, the only reasonable access to the hematoma was the left-sided thoracotomy, which we were able to successfully perform.

CONCLUSIONS

Left-sided aortic aneurysmectomy is a reasonable option to treat bronchial compression after EVAR.

References

1. Parodi JC, Palmaz JC, Barone HD. Transfemoral intraluminal graft implantation for abdominal aortic aneurysms. *Ann Vasc Surg.* 1991;5:491-9.
2. Gopaldas RR, Huh J, Dao TK, LeMaire SA, Chu D, Bakaeen FG, et al. Superior nationwide outcomes of endovascular versus open repair for isolated descending thoracic aortic aneurysm in 11,669 patients. *J Thorac Cardiovasc Surg.* 2010; 140:1001-10.
3. Morales JP, Greenberg RK, Lu Q, Cury M, Hernandez AV, Mohabbat W, et al. Endoleaks following endovascular repair of thoracic aortic aneurysm: etiology and outcomes. *J Endovasc Ther.* 2008;15:631-8.
4. Morales JP, Chan YC, Bell RE, Reidy JF, Taylor PR. Endoluminal repair of distal aortic arch aneurysms causing aorto–vocal syndrome. *Int J Clin Pract.* 2008;62: 1511-4.
5. Madden BP, Loke TK, Sheth AC. Do expandable metallic airway stents have a role in the management of patients with benign tracheobronchial disease? *Ann Thorac Surg.* 2006;82:274-8.

Right ventricular exclusion for a neonatal patient with Ebstein anomaly: A free wall resection of the right ventricle

Takuya Kawabata, MD, PhD, Shingo Kasahara, MD, PhD, Sadahiko Arai, MD, PhD, and Shunji Sano, MD, PhD, Okayama, Japan

The treatment of neonatal patients with severe Ebstein anomaly remains challenging for cardiac surgeons and pediatric cardiologists. The enlarged right side of the heart induces cardiopulmonary dysfunction. Since the first report by Starnes,[1] Reemtsen,[2] and their coworkers, several evolutions of a single ventricular palliative operation have been reported. We herein describe a neonatal patient with Ebstein anomaly who underwent a free wall resection of the right ventricle (RV) in combination with single ventricular palliative surgery.

From the Department of Cardiovascular Surgery, Okayama University Graduate School of Medicine, Dentistry, and Pharmaceutical Sciences, Okayama, Japan.
Disclosures: Authors have nothing to disclose with regard to commercial support.
Received for publication Dec 7, 2010; revisions received May 2, 2011; accepted for publication May 23, 2011; available ahead of print July 1, 2011.
Address for reprints: Takuya Kawabata, MD, PhD, Department of Cardiovascular Surgery, Okayama University Graduate School of Medicine, Dentistry, and Pharmaceutical Sciences, 2-5-1 Shikata, Okayama, 700-8558, Japan (E-mail: ktakuya@pop01.odn.ne.jp).
J Thorac Cardiovasc Surg 2011;142:1582-4
0022-5223/$36.00

doi:10.1016/j.jtcvs.2011.05.019

CLINICAL SUMMARY

A male infant was born at 38 weeks' gestation by normal vaginal delivery with a birth weight of 2.55 kg. Ebstein anomaly was diagnosed by fetal ultrasound cardiography (UCG). Postnatal UCG showed massive tricuspid regurgitation with plastering of the tricuspid septal and posterior leaflets, membranous pulmonary atresia, large atrial septal defect, compression of the left ventricle (LV) by the

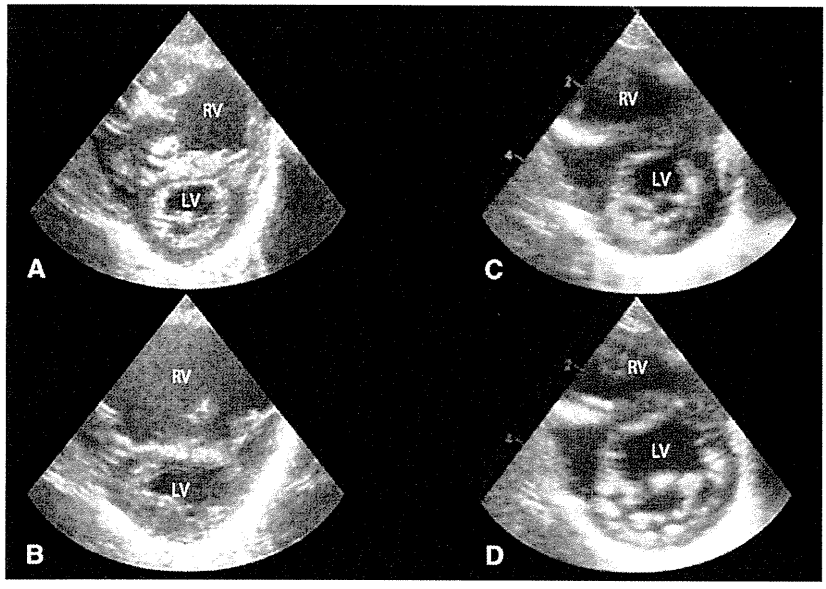

FIGURE 1. A and B, Preoperative echocardiogram in the end-systolic and end-diastolic phases, respectively (short-axis view). The IVS is shifted toward the LV side by the enlarged RV, especially in the end-diastolic phase. C and D, Postoperative echocardiograms in the end-systolic and end-diastolic phases, respectively (short-axis view). The IVS motion becomes normalized and the LV demonstrates a round shape, thus leading to an increase of the LV volume in the end-diastolic phase. *IVS,* Interventricular septum; *LV,* left ventricle; *RV,* right ventricle.

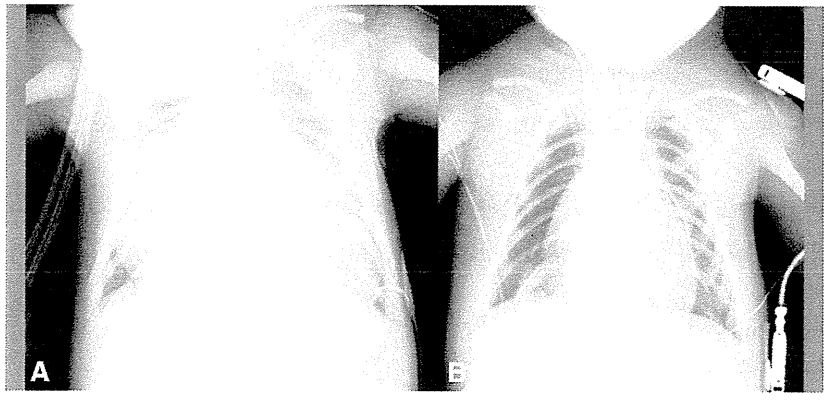

FIGURE 2. A and B, Preoperative and postoperative chest x-ray films, respectively. The cardiothoracic ratio decreased from 0.90 to 0.60. The heart was smaller postoperatively, thus providing the lungs with more space to expand.

enlarged RV, especially in the diastolic phase, and paradoxic motion of the interventricular septum (IVS) (Figure 1, *A* and *B*). The estimated peak RV pressure by tricuspid regurgitation jet was 15 mm Hg and the RV was 1.5 mm in thickness. The Great Ormond Street ratio[3] was 1.6. The cardiothoracic ratio by chest radiography was 0.90 (Figure 2, *A*). He was intubated and lipoprostaglandin E_1 was administered immediately after birth. Pulmonary resistance decreased day by day, and congestive heart failure progressed. Inotropic support and nitrogen inhalation were started on the second and sixth day, respectively. During this period, the repeated UCG did not detect any pulmonary forward flow.

On the seventh day, he underwent a free wall resection of the RV in combination with single ventricular palliative surgery: closure of the tricuspid valve with fenestration, a resection of the RV free wall, and creation of a systemic–pulmonary shunt. Through a median full sternotomy, cardiopulmonary bypass with aortic and bicaval cannulations was established. After cardioplegic cardiac arrest, an oblique right atriotomy was made and the pulmonary atresia was confirmed by direct viewing. Then, the orifice of the tricuspid valve was closed by its leaflets between the anterior and septal leaflets and by an expanded polytetrafluoroethylene patch with a 3.5-mm fenestration between the anterior and posterior leaflets. After release of the aortic crossclamp,

in addition to a free wall resection of the right atrium, the anterior free wall of the thin redundant RV was also resected elliptically and closed directly. The RV wall was thin muscular tissue without fibrosis. The resected area was determined by the RV branch of the right coronary artery and IVS. The procedures were performed with a beating heart to prevent overresection. A systemic–pulmonary shunt was created between the right brachiocephalic artery and the right pulmonary artery with a 3.5-mm expanded polytetrafluoroethylene graft.

On the third postoperative day, delayed sternal closure was carried out. During the operation, additional plications of the RV free wall were performed. After the operation, the cardiothoracic ratio was decreased to 0.60 (Figure 2, *B*), and estimated lung compliance was increased from 2.04 to 2.64 mL/cmH_2O on ventilatory support. Postoperative UCG showed improvement of IVS motion and the LV function (Figure 1, *C* and *D*): the eccentricity index was decreased from 1.85 to 1.16, the end-diastolic volume was increased from 2.4 to 7.0 mL, and the ejection fraction of the LV was increased from 0.45 to 0.78.[4] His postoperative course was uneventful. He has been followed up for 6 months and is currently waiting for a bidirectional cavopulmonary shunt operation.

DISCUSSION

Ebstein anomaly is a rare congenital heart defect of the tricuspid valve and RV; however, several reports have also shown abnormalities of the LV.[2,4] These abnormalities include abnormal motion of the IVS and compression of the LV, which are induced by the enlarged right heart. The enlarged heart also occupies so much space in the thoracic cavity that the lungs are rendered hypoplastic.

Since 1996, to reduce the deleterious effects of the enlarged RV, we have performed free wall resection of the RV for pediatric patients with Ebstein anomaly in combination with one and a half ventricle repair or total cavopulmonary connection.[5] In these patients, the small right heart helps the IVS motion and the LV function to improve and also provides the lungs with more space to expand immediately after the operation. These experiences have therefore led us to indicate this procedure for the neonatal patient.

This is the first published report, to our knowledge, of a neonatal patient with Ebstein anomaly who underwent a free wall resection of the RV in combination with single ventricular palliative surgery.

References

1. Starnes VA, Pitlick PT, Bernstein D, Griffin ML, Choy M, Shumway NE. Ebstein's anomaly appearing in the neonate: a new surgical approach. *J Thorac Cardiovasc Surg*. 1991;101:1082-7.
2. Reemtsen BL, Fagan BT, Wells WJ, Starnes VA. Current surgical therapy for Ebstein anomaly in neonates. *J Thorac Cardiovasc Surg*. 2006;132:1285-90.
3. Shinkawa T, Polimenakos AC, Gomez-Fifer CA, Charpie JR, Hirsch JC, Devaney EJ, et al. Management and long-term outcome of neonatal Ebstein anomaly. *J Thorac Cardiovasc Surg*. 2010;139:354-8.
4. Takagaki M, Ishino K, Kawada M, Ohtsuki S-i, Hirota M, Tanabe Y, et al. Total right ventricular exclusion improves left ventricular function in patients with end-stage congestive right ventricular failure. *Circulation*. 2003;108(suppl II): II226-9.
5. Sano S, Ishino K, Kawada M, Kasahara S, Kohmoto T, Takeuchi M, et al. Total right ventricular exclusion procedure: an operation for isolated congestive right ventricular failure. *J Thorac Cardiovasc Surg*. 2002;123:640-7.

J Physiol Sci (2011) 61:457–465
DOI 10.1007/s12576-011-0166-7

ORIGINAL PAPER

Norwood procedure with non-valved right ventricle to pulmonary artery shunt improves ventricular energetics despite the presence of diastolic regurgitation: a theoretical analysis

Shuji Shimizu · Dai Une · Toshiaki Shishido · Atsunori Kamiya · Toru Kawada · Shunji Sano · Masaru Sugimachi

Received: 17 May 2011 / Accepted: 10 July 2011 / Published online: 10 August 2011

Abstract When the Norwood procedure is conducted for the hypoplastic left heart syndrome using a non-valved right ventricle (RV) to pulmonary artery (PA) shunt, diastolic regurgitation from PA to RV may have an adverse effect on postoperative hemodynamics. In this study, we examined the impact of the diastolic regurgitation on ventricular energetics by computational analysis using a combination of a time-varying elastance chamber model and a modified three-element Windkessel vascular model. This study revealed that use of the valved or non-valved RV-PA shunt eliminated pulmonary over-circulation which was observed when using the systemic to pulmonary artery shunt (modified Blalock–Taussig shunt). Although the valved RV-PA shunt improved pulmonary blood supply and consequently increased pulmonary artery flow and oxygen saturation compared to the non-valved RV-PA shunt, the non-valved RV-PA shunt improved ventricular energetics in spite of the presence of PA to RV regurgitation.

Keywords Hypoplastic left heart syndrome · Norwood procedure · Right ventricle to pulmonary artery shunt · Ventricular energetics · Valved · Computational model

S. Shimizu (✉) · D. Une · T. Shishido · A. Kamiya · T. Kawada · M. Sugimachi
Department of Cardiovascular Dynamics, National Cerebral and Cardiovascular Center Research Institute, 5-7-1 Fujishiro-dai, Suita, Osaka 565-8565, Japan
e-mail: shujismz@ri.ncvc.go.jp

S. Shimizu · S. Sano
Department of Cardiovascular Surgery, Okayama University Graduate School of Medicine, Dentistry and Pharmaceutical Sciences, Okayama, Japan

Introduction

The outcome of the Norwood procedure for hypoplastic left heart syndrome (HLHS) has improved in the past several decades. Previously, pulmonary circulation was maintained by a systemic to pulmonary artery shunt (SPS), such as the modified Blalock–Taussig shunt. However, the SPS has the drawback of systemic-to-pulmonary diastolic run-off, which causes a massive increase in ventricular preload. The development of the right ventricle to pulmonary artery (RV-PA) shunt may have contributed to the dramatic improvement in clinical outcome of recent years, because the RV-PA shunt eliminates the diastolic run-off and increases diastolic systemic arterial pressure (SAP). This increase in diastolic SAP may improve coronary blood supply [1]. Furthermore, the RV-PA shunt may reduce myocardial oxygen demand. Bove et al. [2] reported that the RV-PA shunt decreased stroke work and improved right ventricular energetics.

The RV-PA shunt may be classified into valved and non-valved. The non-valved RV-PA shunt is associated with diastolic regurgitation from PA to RV. This regurgitation may increase RV preload and myocardial oxygen demand compared to the valved RV-PA shunt. Therefore, preventing diastolic regurgitation using the valved conduit may further improve clinical outcome. Reihartz et al. [3] reported that use of a homograft valved RV-PA conduit was associated with low early mortality. Takeuchi et al. [4] used a valved saphenous vein homograft and also reported improved right ventricular function. However, whether the non-valved RV-PA shunt truly improves the outcome of the Norwood procedure compared to the SPS, and whether the valved RV-PA shunt further improves the outcome compared to the non-valved RV-PA shunt remain controversial.

This study aimed to clarify the impact of diastolic regurgitation from PA to RV on ventricular energetics by conducting a theoretical analysis using computational models.

Methods

We modeled the cardiovascular systems of the Norwood procedure using the SPS, and valved and non-valved RV-PA shunts. The electrical analogs of the models used to simulate the cardiovascular systems are shown in Fig. 1. We modeled the postoperative cardiovascular systems mathematically by a combination of the time-varying elastance cardiac chamber model and the three-element Windkessel vascular model.

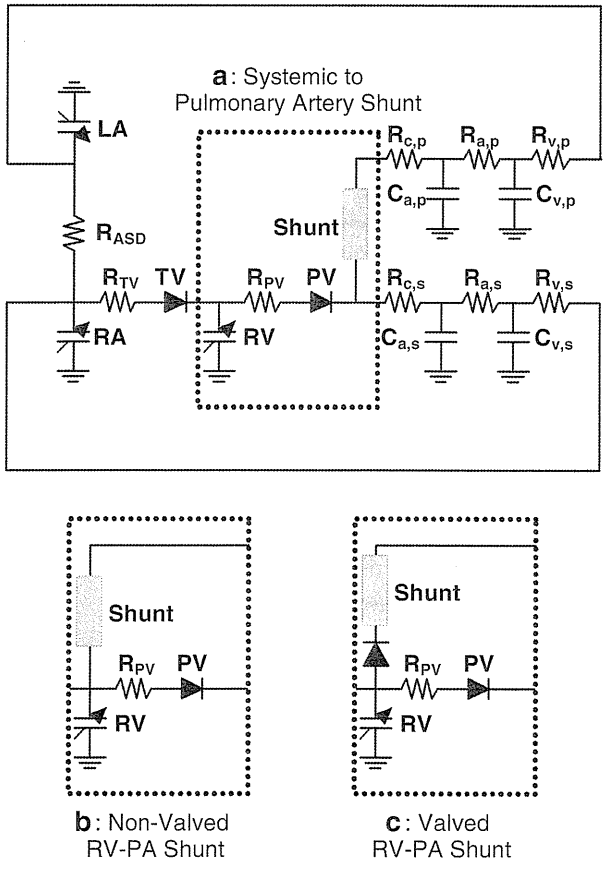

Fig. 1 Electrical analogs of Norwood procedures. **a** Norwood procedure with systemic to pulmonary shunt, **b** Norwood procedure with non-valved right ventricle to pulmonary artery (RV-PA) shunt, **c** Norwood procedure with valved RV-PA shunt. *LA* left atrium, *RA* right atrium, *RV* right ventricle, *PV* pulmonary valve, *TV* tricuspid valve, *ASD* atrial septal defect. R_a arterial resistance, R_c characteristic impedance, R_v venous resistance, C_a arterial capacitance, C_v venous capacitance. *s* and *p* systemic and pulmonary circulation, respectively. R_{PV}, R_{TV} and R_{ASD} resistance at PV, TV and ASD, respectively

Heart

The right ventricular and atrial chambers are represented by the time-varying elastance model [5–7]. The end-systolic pressure–volume relationship is described by a linear equation:

$$P_{es,cc} = E_{es,cc}[V_{es,cc} - V_{0,cc}] \quad (1)$$

where $P_{es,cc}$ is end-systolic pressure, $V_{es,cc}$ is end-systolic volume, $E_{es,cc}$ is the maximal volume elastance, $V_{0,cc}$ is the volume at which end-systolic pressure is equal to 0 mmHg, and cc denotes the right atrial (RA), left atrial (LA), or right ventricular (RV) chamber. The end-diastolic pressure–volume relationship is represented by a non-linear equation:

$$P_{ed,cc} = A_{cc}[e^{B_{cc}(V_{ed,cc}-V_{0,cc})} - 1] \quad (2)$$

where $P_{ed,cc}$ is end-diastolic pressure, $V_{ed,cc}$ is end-diastolic volume, A_{cc} and B_{cc} are constants [5–7]. We assumed the time course of elastance by defining normalized elastance curve $e_{cc}(t)$ as follows:

$$\begin{aligned} e_{cc}(t) &= 0.5\,[1 - \cos(\pi t/T_{es,cc})] \quad (0 \le t < 2T_{es,cc}) \\ e_{cc}(t) &= 0 \quad (2T_{es,cc} \le t < T_c) \end{aligned} \quad (3)$$

where t is the time from the start of systole, $T_{es,cc}$ is the time to the end of systole, and T_c is the duration of cardiac cycle. Using $e_{cc}(t)$, the instantaneous pressure–volume relationship is described by:

$$P_{cc}(t) = [P_{es,cc}(V_{cc}) - P_{ed,cc}(V_{cc})]e_{cc}(t) + P_{ed,cc}(V_{cc}) \quad (4)$$

Ventricular systole is preceded by atrial systole. The time advance of atrial systole (DT) is calculated as a fixed fraction of T_c (DT = 0.02 T_c) [9]. The function of each chamber is characterized by the parameters $E_{es,cc}$, $T_{es,cc}$, $V_{0,cc}$, A_{cc}, B_{cc} and $e_{cc}(t)$. The same $e_{cc}(t)$ is used for all chambers, but the other parameters are different between chambers, as shown in Table 1. Nonrestrictive atrial septal defect is described as constant resistance (R_{ASD}). Each valve is represented as an ideal diode connected serially to a small resistor (pulmonary R_{PV}, tricuspid R_{TV}).

Vascular system

Basically, the pulmonary and systemic circulations are modeled as modified Windkessel impedances. Each vascular system is modeled by lumped venous (C_v) and arterial (C_a) capacitances, a characteristic impedance (R_c) that is related to the stiffness of the proximal aorta or pulmonary artery, a lumped arterial resistance (R_a), and a

Table 1 Parameters used in modeling

Heart rate (HR) (beats/min)	160		
Duration of cardiac cycle (T_c) (ms)	375		
Time to end systole (T_{es}) (ms)	RV: 136	RA: 56	LA: 56
End-systolic elastance (E_{es}) (mmHg/ml)	RV: 8.5	RA: 7.35	LA: 7.35
Scaling factor of EDPVR (A) (mmHg)	RV: 0.9	RA: 0.17	LA: 0.17
Exponent for EDPVR (B) (ml^{-1})	RV: 0.062	RA: 0.484	LA: 0.484
Unstressed volume (V_0) (ml)	RV: 4	RA: 1	LA: 1
Valvular resistance (forward) (mmHg s ml^{-1})	Pulmonary: 0.0004	Tricupsid: 0.00004	
Resistance (mmHg s ml^{-1})	ASD: 0.001		
Index of pure viscous effects (k_1) [mmHg $(l/s)^{-1}$ mm^4]	Shunt: 5.76×10^4		
Index of convective acceleration (k_2) [mmHg $(l/s)^{-2}$ mm^4]	Shunt: 1.87×10^7		
Arterial resistance (R_a) (mmHg s ml^{-1})	Systemic (s): 3.83	Pulmonary (p): 0.63	
Characteristic impedance (R_c) (mmHg s ml^{-1})	Systemic (s): 0.20	Pulmonary (p): 0.028	
Venous resistance (R_v) (mmHg s ml^{-1})	Systemic (s): 0.083	Pulmonary (p): 0.011	
Arterial capacitance (C_a) (ml/mmHg)	Systemic (s): 0.50	Pulmonary (p): 0.31	
Venous capacitance (C_v) (ml/mmHg)	Systemic (s): 4.39	Pulmonary (p): 0.89	

RV right ventricle, *RA* right atrium, *LA* left atrium, *EDPVR* end-diastolic pressure–volume relation, *ASD* atrial septal defect

resistance proximal to C_v (R_v). This framework is similar to that used in deriving Guyton's resistance to venous return [8]. Arterial and venous capacitors for systemic circulation are denoted by $C_{a,s}$ and $C_{v,s}$, respectively, and those for pulmonary circulation by $C_{a,p}$ and $C_{v,p}$. The ratio of C_a to C_v is obtained from previous reports [6, 9, 10].

The relation between pressure (P_c) and volume (V_c) in each capacitance is described by the following linear equation:

$$P_c = \frac{V_c}{C} \tag{5}$$

The change in volume in each capacitance [$dV(t)/dt$] is described by the differential equation below:

$$\frac{dV(t)}{dt} = \sum Q_{inflow}(t) - \sum Q_{outflow}(t) \tag{6}$$

where $Q_{inflow}(t)$ and $Q_{outflow}(t)$ indicate the instantaneous volumetric flow rates at the inlet and outlet, respectively, of each compartment.

Pressure drop across the shunt

Flow of non-Newtonian fluid in a curved pipe is approximated as a quadratic function of $Q(t)$ [11, 12]. The instantaneous pressure drop across the shunt is described by:

$$\Delta P(t) = \frac{k_1 Q(t) + k_2 Q^2(t)}{D^4} \tag{7}$$

where $\Delta P(t)$ (mmHg) is pressure drop across the shunt, $Q(t)$ (l/s) is the instantaneous volume flow rate in shunt, D (mm) is the shunt diameter, k_1 [mmHg $(l/s)^{-1}$ mm^4] is the index of pure viscous effects and k_2 [mmHg $(l/s)^{-2}$ mm^4] is the index of convective acceleration [9].

Protocols

First, the control state was simulated using the 4.0-mm SPS model. Total stressed blood volume (V_s), which is the sum of the stressed volumes in all capacitances and in all chambers, was set as 80 ml.

$$V_s = V_{RV} + V_{LA} + V_{RA} + V_{C_{a,s}} + V_{C_{v,s}} + V_{C_{a,p}} + V_{C_{v,p}} \tag{8}$$

We solved the simultaneous differential equations (Eqs. 1–8) using MATLAB (MathWorks).

Shunt diameter (D) was decreased stepwise from 4.0 to 3.0 mm at decrements of 0.5 mm in the SPS model and increased from 4.0 to 6.0 mm at increments of 1.0 mm in both the valved and non-valved RV-PA shunt models. RV forward flow, systemic and pulmonary flows (Q_s and Q_p), systemic and pulmonary arterial pressures (SAP and PAP), right ventricular end-diastolic volume (RVEDV), stroke work (SW), systolic pressure–volume area (PVA) and mechanical efficiency after each procedure were calculated for each shunt diameter. Heart rate and mean SAP were set at the same values as those of the control state, by adjusting the total stressed blood volume (V_s).

Calculation of arterial and venous oxygen saturation

Since the total amount of O_2 present in the atrium is preserved and the decrease in O_2 content in blood balances the whole body O_2 consumption, arterial (SaO_2) and venous O_2 saturation (SvO_2) are calculated by the following equations for Q_p and Q_s (l/min):

$$SaO_2 = S_{PV}O_2 - \frac{CVO_2 \times BSA}{1.34 \times Hb \times 10 \times Q_p}$$

$$SvO_2 = SaO_2 - \frac{CVO_2 \times BSA}{1.34 \times Hb \times 10 \times Q_s}$$

where $S_{PV}O_2$ is the pulmonary venous O_2 saturation, CVO_2 (ml O_2/min/m^2) is the whole body O_2 consumption, BSA (m^2) is the body surface area, and Hb (g/dl) is the hemoglobin concentration. The constant 10 (dl/l) converts l to dl, and 1.34 (ml O_2/g) converts hemoglobin content to oxygen content. The following assumptions are used in the O_2 calculation: $S_{PV}O_2 = 0.97$ (dimensionless), $CVO_2 = 185$ ml O_2/min/m^2, BSA = 0.20 m^2 and Hb = 16.0 g/dl [9, 13].

Results

The hemodynamic parameters obtained from the computational simulations are shown in Table 2.

Although the increase in shunt diameter caused an increase in systolic SAP and a decrease in diastolic SAP in the SPS model, changes in shunt diameter only affect systolic and diastolic SAP slightly in both the valved and non-valved RV-PA shunt models. Despite the use of small caliber shunt in the SPS model, mean PAP, Q_p and Q_p/Q_s were higher than in both valved and non-valved RV-PA shunt models. Mean PAP, Q_p and Q_p/Q_s in the 3.5-mm SPS model were higher than those in the 6.0-mm non-valved RV-PA shunt model and almost equivalent to those in the 5.0-mm valved RV-PA shunt model.

Right ventricular pressure, SAP, PAP, aortic flow, and shunt flow in the 3.5-mm SPS, 6.0-mm non-valved shunt, and 5.0-mm valved RV-PA shunt models are shown in Fig. 2. In both valved and non-valved RV-PA shunt models, RV ejection to pulmonary circulation through the shunt preceded RV ejection to systemic circulation and continued even after the end of ejection to systemic circulation. Comparisons of the hemodynamics of the 3.5-mm SPS, and 5.0-mm valved and 6.0-mm non-valved RV-PA shunt models are shown in Fig. 3. RVEDV was smaller in the 6.0-mm non-valved RV-PA shunt (−3.7%) and the 5.0-mm valved RV-PA shunt (−11.7%) models than that in the 3.5-mm SPS model. At the same shunt diameter, mean PAP, Q_p, Q_p/Q_s, SaO_2 and SvO_2 were higher with the valved RV-PA shunt than with the non-valved shunt.

In the SPS model, the use of a larger conduit significantly increased systemic-to-pulmonary diastolic run-off and RVEDV (Table 2). In the valved and non-valved RV-PA shunt models, increase in conduit size likewise

Table 2 Hemodynamic data obtained from computational simulation of SPS, non-valved RV-PA shunt, and valved RV-PA shunt

	Mathematical models								
	SPS			Non-valved RV-PA			Valved RV-PA		
Shunt diameter (mm)	3.0	3.5	4.0	4.0	5.0	6.0	4.0	5.0	6.0
Heart rate (beats/min)	160			160			160		
Systolic systemic artery pressure (mmHg)	83.9	87.0	90.9	75.7	76.3	77.0	75.7	76.2	76.9
Diastolic systemic artery pressure (mmHg)	46.6	45.0	43.4	51.9	51.9	51.9	51.9	51.8	51.9
Mean systemic artery pressure (mmHg)	58.6	58.7	58.7	58.7	58.7	58.7	58.7	58.7	58.7
Mean PA pressure (mmHg)	10.4	13.8	17.3	7.50	9.83	11.9	8.98	12.6	16.2
RV forward flow (l/min)	1.60	1.86	2.14	1.53	1.86	2.19	1.51	1.81	2.10
Q_p (l/min)	0.77	1.04	1.32	0.55	0.73	0.90	0.68	0.98	1.27
Q_s (l/min)	0.83	0.82	0.82	0.83	0.83	0.83	0.83	0.83	0.83
Q_p/Q_s	0.94	1.26	1.62	0.66	0.88	1.09	0.81	1.18	1.54
Diastolic run-off (l/min)	0.52	0.69	0.85						
Diastolic regurgitation (l/min)				0.15	0.29	0.47			
SaO_2 (%)	74.7	80.4	83.9	65.4	73.5	77.8	71.5	79.3	83.4
SvO_2 (%)	53.9	59.5	62.8	44.8	52.8	56.9	50.8	58.5	62.5
Stressed blood volume (ml)	70.6	75.1	80.0	64.9	67.9	71.4	65.7	69.2	73.2
RVEDV (ml)	21.6	23.3	25.0	19.4	20.8	22.4	19.3	20.6	22.0
Stroke work (mmHg ml)	759	905	1,062	600	713	829	596	704	815
Systolic PVA (mmHg ml)	1,008	1,157	1,315	765	851	949	762	843	934
Mechanical efficiency (%)	75.3	78.2	80.8	78.4	83.8	87.4	78.3	83.5	87.2

SPS systemic to pulmonary artery shunt, *RV-PA* right ventricle to pulmonary artery shunt, *RV* right ventricle, *PA* pulmonary artery, Q_p pulmonary blood flow, Q_s systemic blood flow, SaO_2 arterial oxygen saturation, SvO_2 venous oxygen saturation, *RVEDV* right ventricular end-diastolic volume, *PVA* systolic pressure–volume area

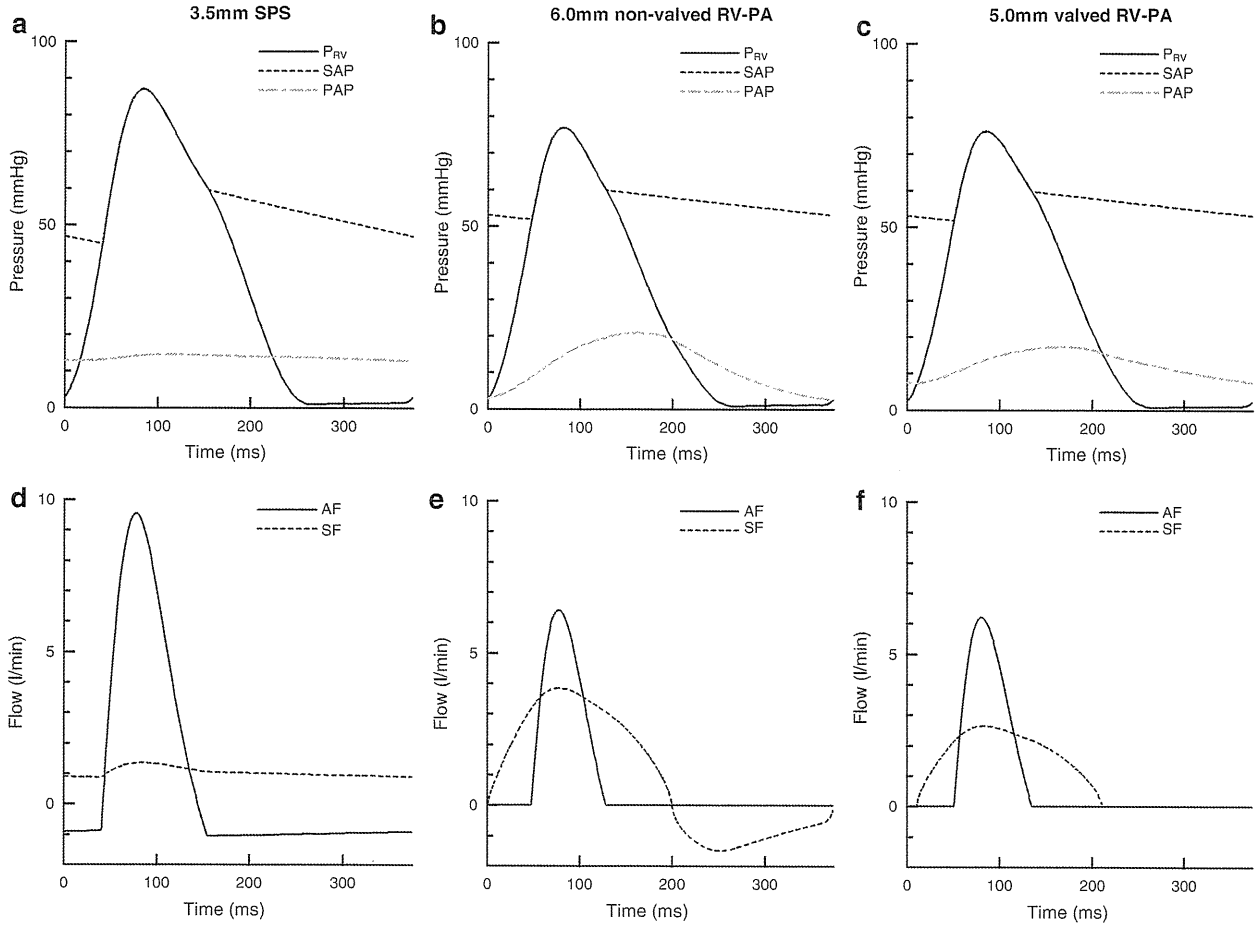

Fig. 2 Right ventricular pressure, systemic and pulmonary arterial pressures, aortic flow and shunt flow computed from the mathematical models of Norwood procedures with 3.5-mm systemic to pulmonary artery shunt (SPS **a**, **d**), 6.0-mm non-valved right ventricle to pulmonary artery (RV-PA) shunt (**b**, **e**), and 5.0-mm valved RV-PA shunt (**c**, **f**). P_{RV} right ventricular pressure, SAP systemic arterial pressure, PAP pulmonary arterial pressure, AF aortic flow, SF shunt flow

increased RVEDV, but the magnitudes were smaller than those of the SPS model, despite larger conduits being used in these models. The smaller RVEDV contributed to decreases in SW and PVA. The pressure–volume loops of the 3.5-mm SPS, and the 5.0-mm valved and 6.0-mm non-valved RV-PA shunt models are shown in Fig. 4. The SW in the 5.0-mm valved and 6.0-mm non-valved RV-PA shunts were −22.3 and −8.4%, respectively, smaller than that in the 3.5-mm SPS. The PVA in the 5.0-mm valved and 6.0-mm non-valved RV-PA shunts were −27.1 and −18.0%, respectively, smaller than that in the 3.5-mm SPS. Mechanical efficiency (SW/PVA) in the 5.0-mm valved and 6.0-mm non-valved RV-PA shunt were 5.3 and 9.2%, respectively, higher than that in the 3.5-mm SPS. Although the use of non-valved conduit caused diastolic regurgitation from PA to RV, there was no difference in mechanical efficiency between the valved and non-valved RV-PA shunts at the same shunt diameter. Furthermore, compared to the SPS and the valved RV-PA shunt, the non-valved RV-PA shunt delivered the highest mechanical efficiency at any given Q_p/Q_s (Fig. 5).

Discussion

The Norwood procedure for stage I palliation of the HLHS was first reported in 1983 [14]. In the conventional Norwood procedure, pulmonary circulation was maintained by a SPS, such as the modified Blalock–Taussig shunt. The development of the RV-PA shunt in the last decade has improved patient's mortality and morbidity [15]. Since Sano et al. [16] reported their experience with the non-valved RV-PA shunt in 2003, this modification has been widely used. However, it remains controversial whether the RV-PA shunt truly improves the outcome of the Norwood procedure.

The RV-PA shunt eliminates systemic to pulmonary diastolic run-off that occurs when using the SPS, which

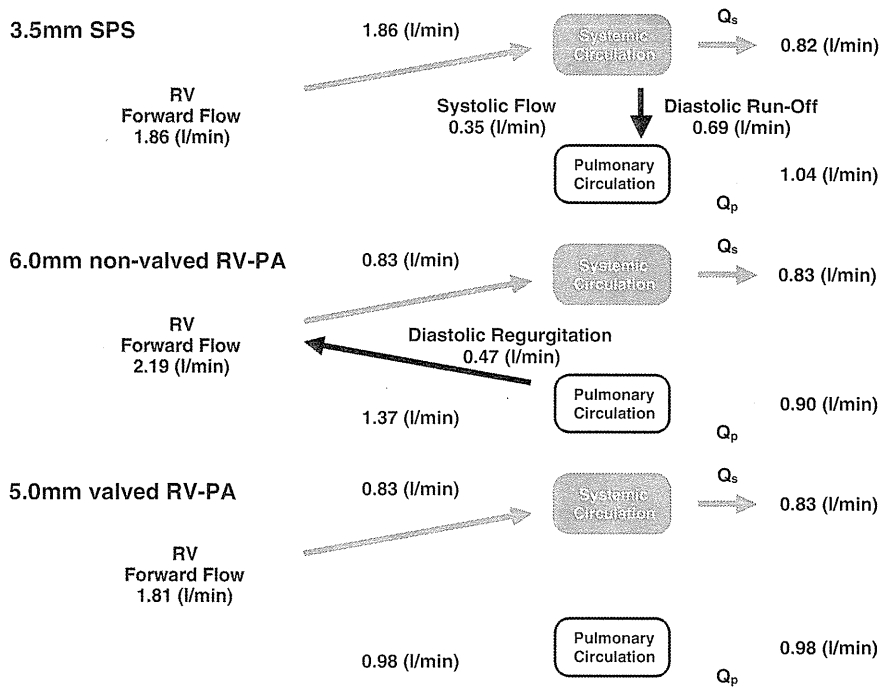

Fig. 3 Hemodynamics obtained from the 3.5-mm systemic-to-pulmonary shunt (*SPS*) model, and 6.0-mm non-valved and 5.0-mm valved right ventricle to pulmonary artery (*RV-PA*) shunt models

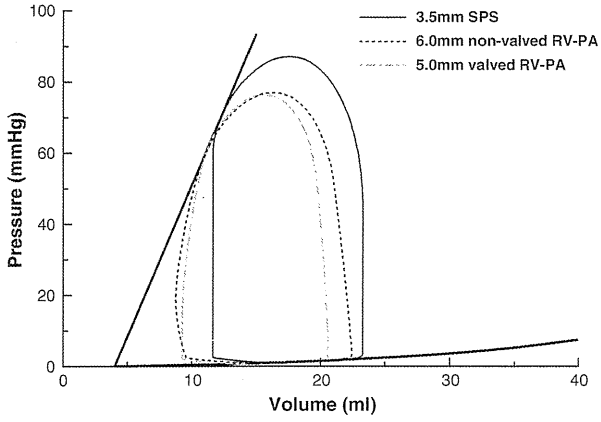

Fig. 4 Pressure-volume loops of simulated Norwood procedures. *Solid line* 3.5-mm systemic to pulmonary artery shunt (SPS), *dotted line* 6.0-mm non-valved right ventricle to pulmonary artery (RV-PA) shunt, *dot-dashed line* 5.0-mm valved RV-PA shunt

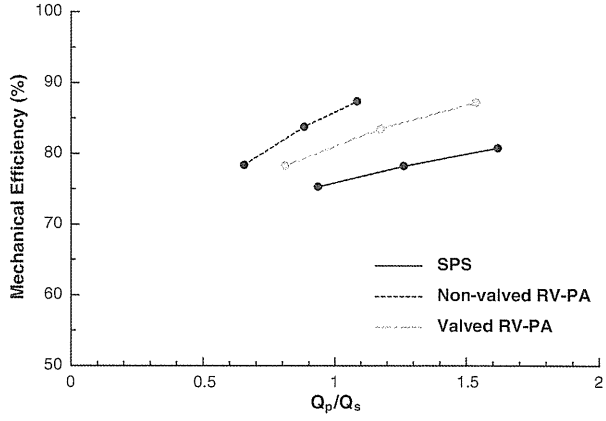

Fig. 5 The relation between Q_p/Q_s and mechanical efficiency. *Solid line* systemic to pulmonary artery shunt (SPS), *dotted line* non-valved right ventricle to pulmonary artery (RV-PA) shunt, *dot-dashed line* valved RV-PA shunt

causes a massive increase in ventricular preload. However, diastolic regurgitation from PA to RV is a drawback of the non-valved RV-PA shunt. Thus, some authors have reported the advantages of a valved RV-PA shunt [3, 4, 17]. Use of a valved RV-PA shunt prevents diastolic regurgitation from PA to RV, and should further decrease ventricular preload. However, the present theoretical study based on mathematical models revealed that the valved RV-PA shunt mainly improves pulmonary blood supply and the favorable effect on ventricular energetics is equivalent to that of the non-valved RV-PA shunt.

Influence on systemic circulation

In the SPS model, the use of a larger caliber shunt increased systolic SAP and decreased diastolic SAP. In both the valved and non-valved RV-PA shunt models, however, systolic and diastolic SAP did not change with the increase in shunt diameter. Diastolic SAP in both RV-PA shunt models were at most 8 mmHg higher than that in the SPS model. Some clinical reports have already demonstrated lower diastolic SAP using the SPS [18, 19]. Lower diastolic SAP may decrease coronary perfusion

pressure and result in coronary malperfusion. Therefore, excessive decrease in diastolic SAP when using the SPS may cause global myocardial ischemia and impair the postoperative surgical outcome. On the other hand, higher and stable diastolic SAP with both the valved and non-valved RV-PA shunts is favorable for myocardial blood supply.

Influence on pulmonary circulation

The Q_p was excessively high in the SPS model, but was lower in both the valved and non-valved RV-PA shunt models. The Q_p in the 3.5-mm SPS model was similar to that in the 5.0-mm valved RV-PA shunt and higher than that in the 6.0-mm non-valved RV-PA shunt model. The RV-PA shunts contributed to avoiding pulmonary over-circulation and maintaining appropriate pulmonary blood supply in spite of the larger conduits.

In the present study, the valved RV-PA shunt eliminated diastolic regurgitation from PA to RV, and improved pulmonary blood supply compared to the non-valved RV-PA shunt. At the same shunt diameter, Q_p was at most 42% higher in the valved RV-PA shunt than in the non-valved RV-PA shunt model. This resulted in higher oxygen saturation in the valved RV-PA shunt. To obtain the same Q_p as the valved RV-PA shunt, a non-valved RV-PA shunt may require larger stressed blood volume and may cause the increase in ventricular preload. Since some authors reported decreased SvO_2 as a predictor of morbidity after the Norwood procedure [20, 21], the valved RV-PA shunt that yields higher SvO_2 may be favorable for pulmonary circulation.

Caspi et al. [22] suggested that the Norwood procedure with RV-PA conduit may have favorable effects on the development of the pulmonary artery, which may be associated with the pulsatile pulmonary flow. The importance of pulsatility for the growth of pulmonary artery has been reported [23, 24]. The smaller pulsatility of pulmonary flow in the SPS as shown in Fig. 2d may impair the development of the pulmonary artery.

Influence on RVEDV

The RVEDV was markedly reduced in both the non-valved and valved RV-PA shunt models compared to the SPS model. When using a SPS, systemic and pulmonary arteries are directly connected. Therefore, a blood shift from systemic to pulmonary circulation in the diastolic phase (diastolic run-off) cannot be avoided, because pulmonary vascular resistance is usually lower than systemic vascular resistance. This should cause a decrease in systemic arterial pressure and require a greater stressed blood volume to maintain the mean SAP (Table 2), resulting in increased RVEDV and Q_p. When the RV-PA shunts are used, since systemic and pulmonary arteries originate separately from the RV, diastolic run-off is avoided and RVEDV and Q_p are lower as a result. The lower RVEDV contributes to improvement of ventricular energetics as described below.

Influence on ventricular energetics

Diastolic regurgitation from PA to RV occurs when a non-valved RV-PA shunt is used. It is possible that the diastolic regurgitation may increase ventricular preload and impair ventricular energetics compared to the valved RV-PA shunt. However, the present study demonstrated that use of both the valved and non-valved RV-PA shunts eliminated systemic to pulmonary diastolic run-off and improved mechanical efficiency (SW/PVA) to the same extent. Compared to the 3.5-mm SPS model, the lower RVEDV in both the 5.0-mm valved and 6.0 mm non-valved RV-PA shunt models contributed to decreasing PVA (−27.2 and −18.0%, respectively) and increasing mechanical efficiency (+5.3 and +9.2%, respectively). Therefore, the influence of diastolic regurgitation associated with the non-valved RV-PA shunt may be small from the viewpoint of ventricular energetics. Because PVA correlates significantly with myocardial oxygen consumption [24], decreased PVA results in reduced myocardial oxygen demand. The present results suggest that both RV-PA shunts reduce myocardial oxygen demand.

This advantage of both RV-PA shunts in ventricular energetics may be associated with the RV ejection pattern through the RV-PA shunts. With the SPS, RV has to pump the blood to a higher pressure system i.e., the systemic circulation. This limits the duration of RV ejection and requires higher RV systolic pressure. However, with both the RV-PA shunts, the systemic and pulmonary arteries originate separately from the RV. The RV ejects blood steadily via the RV-PA shunt to the pulmonary circulation that has a relatively low pressure (Fig. 2). This fact may contribute to the decreased SW and PVA when using the valved and non-valved RV-PA shunts.

Advantage of RV-PA shunt

The higher diastolic SAP obtained from using a RV-PA shunt has been reported to improve coronary blood supply [1]. However, under physiological conditions, coronary blood flow depends on myocardial oxygen demand [25]. The greatest advantage of the RV-PA shunt is that this procedure decreases myocardial oxygen demand through decreasing PVA. The RV-PA shunt is able to maintain systemic circulation at lower oxygen consumption compared to the SPS, implying that the RV-PA shunt requires less coronary blood flow than the SPS to maintain the same

Table 3 The influence of ventriculotomy on ventricular energetics

	$E_{es,RV}$ (mmHg/ml)	SW (mmHg ml)	PVA (mmHg ml)	Mechanical efficiency (%)
3.5-mm SPS	8.5	905	1,157	78.2
6.0-mm non-valved RV-PA	7.5	827	977	84.7
	6.5	825	1,018	81.1
5.0-mm valved RV-PA	7.5	702	875	80.3
	6.5	698	916	76.2

SPS systemic to pulmonary artery shunt, *RV-PA* right ventricle to pulmonary artery shunt, $E_{es,RV}$ end-systolic elastance of right ventricle, *SW* stroke work, *PVA* systolic pressure–volume area

systemic circulation. This feature may contribute to the improvement of coronary flow reserve. The RV-PA shunt may have better tolerance to the postoperative myocardial ischemia.

Limitations

The present study had some limitations. First, the potential damage of right ventriculotomy was disregarded in the present simulations. Ventricular incision is required to place the valved or non-valved RV-PA shunt. Although ventriculotomy may cause ventricular systolic dysfunction or tricuspid regurgitation, Graham et al. [26] observed no apparent deleterious effects of right ventriculotomy following the Norwood procedure using a RV-PA shunt. Furthermore, our additional simulation suggested that the RV-PA shunt still improved ventricular energetics in spite of the potential damage of ventriculotomy, which decreased the end-systolic elastance of RV ($E_{es,RV}$) from 8.5 to 7.5 mmHg/ml (Table 3). However, mechanical efficiency in the 5.0-mm valved RV-PA shunt would be lower than that in the 3.5-mm SPS when ventriculotomy decreased $E_{es,RV}$ to 6.5 mmHg/ml.

Second, systemic and pulmonary vascular resistance did not change in the present simulations. Vascular resistance was the same in all three shunt models. The differences in pulsatility of the three procedures may affect vascular resistance. A previous report indicated that a sudden increase in systemic vascular resistance caused circulatory collapse in Norwood patients [27]. Therefore, further analyses on the influence of vascular resistance are required.

Third, inertial effects in the shunt were disregarded in the present study. If we considered flow in the shunt as unsteady flow, inertial effects would have a great impact on the pressure-drop across the shunt. [28] Then, the length of shunt might become a strong determinant of pressure–flow relationship.

Conclusions

The present theoretical analysis indicates that both the valved and non-valved RV-PA shunts maintain adequate pulmonary circulation; as a result, the RV delivers greater SW for a lower PVA, i.e., lower myocardial oxygen consumption. Although the valved RV-PA shunt improves pulmonary blood supply and consequently increases Q_p and oxygen saturation compared to the non-valved RV-PA shunt, the favorable effects of the two RV-PA shunts on ventricular energetics are equivalent. The non-valved RV-PA shunt reduces PVA and improves mechanical efficiency in spite of the presence of PA to RV regurgitation.

Acknowledgments This study was supported by a research project promoted by the Japanese Ministry of Health, Labour and Welfare (H20-katsudo-Shitei-007 and H21-nano-Ippan-005); Grants-in-Aid for Scientific Research (No. 20390462, No. 22791328 and No. 23390415) from the Ministry of Education, Culture, Sports, Science and Technology; and the Industrial Technology Research Grant Program from New Energy and Industrial Technology Development Organization (NEDO) of Japan.

References

1. Maher KO, Pizarro C, Gidding SS, Januszewska K, Malec E, Norwood WI Jr, Murphy JD (2003) Hemodynamic profile after the Norwood procedure with right ventricle to pulmonary artery conduit. Circulation 108:782–784
2. Bove EL, Migliavacca F, de Leval MR, Balossino R, Pennati G, Lloyd TR, Khambadkone S, Hsia TY, Dubini G (2008) Use of mathematic modeling to compare and predict hemodynamic effects of the modified Blalock–Taussig and right ventricle-pulmonary artery shunts for hypoplastic left heart syndrome. J Thorac Cardiovasc Surg 136:312–320.e2
3. Reinhartz O, Reddy VM, Petrossian E, MacDonald M, Lamberti JJ, Roth SJ, Wright GE, Perry SB, Suleman S, Hanley FL (2006) Homograft valved right ventricle to pulmonary artery conduit as a modification of the Norwood procedure. Circulation 114:I594–I599
4. Takeuchi K, Murakami A, Takaoka T, Takamoto S (2006) Evaluation of valved saphenous vein homograft as right ventricle-pulmonary artery conduit in modified stage I Norwood operation. Interact Cardiovasc Thorac Surg 5:345–348
5. Burkhoff D, Tyberg JV (1993) Why does pulmonary venous pressure rise after onset of LV dysfunction: a theoretical analysis. Am J Physiol 265:H1819–H1828
6. Morley D, Litwak K, Ferber P, Spence P, Dowling R, Meyns B, Griffith B, Burkhoff D (2007) Hemodynamic effects of partial ventricular support in chronic heart failure: results of simulation validated with in vivo data. J Thorac Cardiovasc Surg 133:21–28
7. Shimizu S, Shishido T, Une D, Kamiya A, Kawada T, Sano S, Sugimachi M (2010) Right ventricular stiffness constant as a predictor of postoperative hemodynamics in patients with

hypoplastic right ventricle: a theoretical analysis. J Physiol Sci 60:205–212
8. Sagawa K, Maughan L, Suga H, Sunagawa K (1988) Cardiovascular interaction. In: Sagawa K, Maughan L, Suga H, Sunagawa K (eds) Cardiac contraction and the pressure–volume relationship. Oxford University Press, Oxford
9. Migliavacca F, Pennati G, Dubini G, Fumero R, Pietrabissa R, Urcelay G, Bove EL, Hsia TY, de Leval MR (2001) Modeling of the Norwood circulation: effects of shunt size, vascular resistances, and heart rate. Am J Physiol Heart Circ Physiol 280:H2076–H2086
10. Huikeshoven F, Coleman TG, Jongsma HW (1980) Mathematical model of the fetal cardiovascular system: the uncontrolled case. Am J Physiol 239:R317–R325
11. Migliavacca F, Dubini G, Pennati G, Pietrabissa R, Fumero R, Hsia TY, de Leval MR (2000) Computational model of the fluid dynamics in systemic-to-pulmonary shunts. J Biomech 33:549–557
12. Young DF, Tsai FY (1973) Flow characteristics in models of arterial stenoses. I. Steady flow. J Biomech 6:395–410
13. Chang AC, Kulik TJ, Hickey PR, Wessel DL (1993) Real-time gas-exchange measurement of oxygen consumption in neonates and infants after cardiac surgery. Crit Care Med 21:1369–1375
14. Norwood WI, Lang P, Hansen DD (1983) Physiologic repair of aortic atresia-hypoplastic left heart syndrome. N Engl J Med 308:23–26
15. Pizarro C, Malec E, Maher KO, Januszewska K, Gidding SS, Murdison KA, Baffa JM, Norwood WI (2003) Right ventricle to pulmonary artery conduit improves outcome after stage I Norwood for hypoplastic left heart syndrome. Circulation 108:II155–II160
16. Sano S, Ishino K, Kawada M, Arai S, Kasahara S, Asai T, Masuda Z, Takeuchi M, Ohtsuki S (2003) Right ventricle-pulmonary artery shunt in first-stage palliation of hypoplastic left heart syndrome. J Thorac Cardiovasc Surg 126:504–509
17. Yamashiro M, Morita K, Uno Y, Shinohara G, Hashimoto K (2011) Modified Norwood procedure with a handmade downsizing valved right ventricle-to-pulmonary artery conduit. Gen Thorac Cardiovasc Surg 59:30–33
18. Bradley SM, Simsic JM, McQuinn TC, Habib DM, Shirali GS, Atz AM (2004) Hemodynamic status after the Norwood procedure: a comparison of right ventricle-to-pulmonary artery connection versus modified Blalock–Taussig shunt. Ann Thorac Surg 78:933–941
19. Azakie A, Martinez D, Sapru A, Fineman J, Teitel D, Karl TR (2004) Impact of right ventricle to pulmonary artery conduit on outcome of the modified Norwood procedure. Ann Thorac Surg 77:1727–1733
20. Hoffman GM, Ghanayem NS, Kampine JM, Berger S, Mussatto KA, Litwin SB, Tweddell JS (2000) Venous saturation and the anaerobic threshold in neonates after the Norwood procedure for hypoplastic left heart syndrome. Ann Thorac Surg 70:1515–1520
21. Hoffman GM, Tweddell JS, Ghanayem NS, Mussatto KA, Stuth EA, Jaquis RD, Berger S (2004) Alteration of the critical arteriovenous oxygen saturation relationship by sustained afterload reduction after the Norwood procedure. J Thorac Cardiovasc Surg 127:738–745
22. Caspi J, Pettitt TW, Mulder T, Stopa A (2008) Development of the pulmonary arteries after the Norwood procedure: comparison between Blalock–Taussig shunt and right ventricular-pulmonary artery conduit. Ann Thorac Surg 86:1299–1304
23. Malec E, Januszewska K, Kolcz J, Mroczek T (2003) Right ventricle-to-pulmonary artery shunt versus modified Blalock–Taussig shunt in the Norwood procedure for hypoplastic left heart syndrome—influence on early and late haemodynamic status. Eur J Cardiothorac Surg 23:728–733
24. Suga H, Yasumura Y, Nozawa T, Futaki S, Igarashi Y, Goto Y (1987) Prospective prediction of O_2 consumption from pressure-volume area in dog hearts. Am J Physiol 252:H1258–H1264
25. Tune JD, Gorman MW, Feigl EO (2004) Matching coronary blood flow to myocardial oxygen consumption. J Appl Physiol 97:404–415
26. Graham EM, Atz AM, Bradley SM, Scheurer MA, Bandisode VM, Laudito A, Shirali GS (2007) Does a ventriculotomy have deleterious effects following palliation in the Norwood procedure using a shunt placed from the right ventricle to the pulmonary arteries? Cardiol Young 17:145–150
27. Wright GE, Crowley DC, Charpie JR, Ohye RG, Bove EL, Kulik TJ (2004) High systemic vascular resistance and sudden cardiovascular collapse in recovering Norwood patients. Ann Thorac Surg 77:48–52
28. Young DF, Tsai FY (1973) Flow characteristics in models of arterial stenoses. II. Unsteady flow. J Biomech 6:547–559